

to force this guest molecule to assume an orientational distribution which is locally very anisotropic is certainly rather surprising if one takes into account the emphasis so far put on the inner disorder of the micellar aggregate.^{2,3}

The intercalation of Orange Red within the host aggregates, perpendicular to their surfaces, is expected to be strongly stabilized by its highly anisotropic molecular shape and also by its ability to grasp at the polar micelle surface through its terminal dimethylamino group.¹

In search for orientational effects in micellar catalysis⁴ and in the hope that the control of stereochemistry by micelles will be more efficient in the future, the use of the LD technique may drive

a true molecular-engineering approach to the reactivity and photochemistry in micellar aggregates.

It is of significance for photochemical applications of photo-selection processes within micellar hosts that the *macroscopic linear anisotropy is highest within N_D^+ micelles*. This provides the way in oriented lyotropic media to make the best use of the intrinsic anisotropy of the photochemical processes.⁴

Acknowledgment. This research was supported by CNR and MPI grants.

Registry No. KL, 10124-65-9; KH_xOB, 108836-72-2; KH_pOB, 96339-97-8; SdS, 142-87-0; dOH, 112-30-1; Orange Red, 2491-74-9.

Extending Surface-Enhanced Raman Spectroscopy to Transition-Metal Surfaces: Carbon Monoxide Adsorption and Electrooxidation on Platinum- and Palladium-Coated Gold Electrodes

Lam-Wing H. Leung and Michael J. Weaver*

Contribution from the Department of Chemistry, Purdue University, West Lafayette, Indiana 47907. Received February 19, 1987

Abstract: Thin (ca. one to three monolayers) films of platinum and palladium electrodeposited on electrochemically roughened gold are observed to yield surface-enhanced Raman (SER) spectra for adsorbed carbon monoxide. The major vibrational band(s) on these surfaces are diagnosed from their frequencies as arising from C–O stretching vibrations, ν_{CO} , for CO bound to the transition-metal overlayers rather than to residual gold sites. The observed SER ν_{CO} frequencies are closely similar to (within ca. 10 cm^{-1}) those obtained for these systems from potential-difference infrared (PDIR) spectra. The major SERS and PDIR ν_{CO} features for the platinum and palladium surfaces appear at 2060–2090 and 1965–1985 cm^{-1} , respectively, consistent with the presence of “terminal” and “bridging” CO on these two electrodes. The infrared as well as electrochemical properties of these systems are closely similar to those for the corresponding polycrystalline “bulk” electrodes. A difference between the SER- and IR-active adsorbed CO, however, is that the former undergoes electrooxidation on both surfaces at 0.2–0.3 V higher overpotentials than the latter form. Examination of the potential-dependent SERS bands for metal oxide vibrations, ν_{PtO} , on the platinum surface shows that the electrooxidation potential for the SERS-active adsorbed CO coincides with that for the appearance of the ν_{PtO} band. Some broader implications to the utilization of SERS for examining transition-metal surfaces are pointed out.

Surface-enhanced Raman scattering (SERS) is now well established as a means of obtaining detailed information for a wide variety of adsorbates, especially in electrochemical environments.¹ However, despite the significant number of metals that have been predicted and/or demonstrated to yield the SERS effect, in practice this technique has been limited almost entirely to silver, gold, and copper surfaces.¹ While these metals, especially gold, are of considerable electrochemical significance, it is clearly of importance to develop means of extending the applicability of SERS to other surfaces.

One possible approach involves coating SERS-active metals with thin overlayers so that the chemical properties of the modified surface reflect primarily that of the overlayer material, yet maintaining SERS activity for species adsorbed on the overlayer by keeping them in suitably close proximity to the underlying substrate. We have recently demonstrated that underpotential deposited (upd) monolayers of mercury, thallium, and lead on electrochemically roughened gold electrodes yield surfaces displaying strong SERS activity for several adsorbates that are bound to the overlayer metal.² This behavior is comparable to that

observed for adsorbates at upd monolayers of silver and copper on gold.³ Gold provides an especially suitable substrate for this purpose from several standpoints. These include the availability of an electrochemical roughening procedure that yields especially stable as well as intense SERS,⁴ the wide potential ranges that are amenable to study using gold, and the high stability of upd and other metallic deposits on this metal.

Given the importance of transition metals in surface chemistry, it is clearly of interest to ascertain if this approach can be utilized to examine SERS at surfaces formed by overlayers of such materials on gold. The electrodeposition of very thin transition-metal layers on noble metal substrates, including gold, has been the subject of a number of investigations, focusing on the electro-sorptive and electrocatalytic properties of the resulting overlayer surfaces.⁵ Overall, these studies show that the electrochemical properties of the metal overlayers mimic those for bulk electrodes of the deposited metal, even for film thicknesses down to one to two equivalent monolayers.⁵

(3) Leung, L.-W. H.; Gosztola, D.; Weaver, M. J. *Langmuir* **1987**, *3*, 45.

(4) (a) Gao, P.; Patterson, M. L.; Tadayoni, M. A.; Weaver, M. J. *Langmuir* **1985**, *1*, 173. (b) Gao, P.; Gosztola, D.; Leung, L.-W. H.; Weaver, M. J. *J. Electroanal. Chem.*, in press.

(5) (a) Rand, D. A. J.; Woods, R. J. *Electroanal. Chem.* **1973**, *44*, 83. (b) Furuya, N.; Motoo, S. *Ibid.* **1978**, *88*, 151. (c) Motoo, S.; Shibata, M.; Watanabe, M. *Ibid.* **1983**, *110*, 103. (d) Lin-Cai, J.; Pletcher, D. *Ibid.* **1983**, *149*, 237.

(1) Recent reviews include: (a) Chang, R. K.; Laube, B. L. *CRC Crit. Rev. Solid State Mater. Sci.* **1984**, *12*, 1. (b) Moskovits, M. *Rev. Mod. Phys.* **1985**, *57*, 783. (c) Weitz, D. A.; Moskovits, M.; Creighton, J. A. In *Chemistry and Structure at Interfaces — New Laser and Optical Techniques*; Hall, R. B., Ellis, A. B., Eds.; VCH Publishers: Deerfield Beach, FL, 1986; p 197.

(2) Leung, L.-W. H.; Weaver, M. J. *J. Electroanal. Chem.* **1987**, *217*, 367.

We have recently found that such ultrathin layers of transition metals on electrochemically roughened (i.e., SERS-active) gold including platinum, palladium, rhodium, and ruthenium, yield observable and even intense SERS for small molecules such as carbon monoxide, alkenes, and alkynes. Of these adsorbates, CO provides a valuable model system in view of the well-known sensitivity of the C–O stretching frequency, ν_{CO} , to the surface environment, especially the chemical nature of the metal.⁴ Consequently, the observed ν_{CO} frequencies provide a ready means of distinguishing between SERS arising from CO molecules bound to the overlayer metal rather than to residual gold sites. We have previously examined the adsorption and electrooxidation of CO on gold by using SERS.⁷

This initial communication of these findings summarizes representative results that we have obtained so far for SERS of CO adsorbed on platinum- and palladium-coated gold surfaces. Parallel surface infrared data are also presented for these systems, using a potential-difference technique to subtract out interference by the bulk solution.⁸ Such comparisons between surface infrared and Raman spectra provide a means of ascertaining the vibrational properties of the SERS-active species with respect to those of the preponderant adsorbate that is presumably sensed by the infrared probe.⁹ We also consider here the electrooxidation of adsorbed CO on these surfaces as monitored by the potential-dependent Raman and infrared spectra. Besides the bands associated with adsorbed CO, the platinum overlayer surface yields metal–oxygen Raman vibrations, ν_{PtO} , associated with transition metal oxide formation, similarly to that observed on unmodified gold electrodes.¹⁰ The comparison between the potential-dependent intensities of the ν_{CO} and ν_{PtO} vibrations yields some insight into the nature of the electrooxidation mechanism.

Experimental Section

Most details of the laser Raman system used for the electrochemical SERS measurements are as described elsewhere.¹¹ Laser excitation was provided by a Spectra-Physics Model 165 Kr⁺ laser operated at 647.1 nm, with a power of about 50–80 mW spot focused on the electrode surface. The Raman scattered light was collected using a 50-mm diameter *f*/0.95 camera lens (DO Industries Model DO-5095) into a SPEX Model 1403 scanning spectrometer. Details of the surface infrared measurements are given in ref 12. The infrared spectrometer was a Bruker-IBM IR 98-4A Fourier transform instrument, with a globar light source and a liquid-nitrogen cooled MCT narrow-band detector (Infrared Associates Model HCT-18A).

The gold electrode used for the SERS measurements was a 4-mm diameter disk sheathed in Teflon. A somewhat larger, 9-mm diameter, electrode was used for the surface infrared measurements to accommodate the IR light beam. The latter was utilized in a thin-layer geometry, formed by pushing the electrode up to the calcium fluoride window. After mechanical polishing the electrodes were electrochemically roughened, so as to yield SERS activity, by means of oxidation–reduction cycles in 0.1 M KCl as described in ref 4 and 10, followed by rinsing and transferred successively to the electrodeposition and spectroelectrochemical cells.

The electrodeposition of the platinum and palladium (see Results section) employed hydrogen hexachloroplatinate(IV) ($\text{H}_2\text{PtCl}_6 \cdot x\text{H}_2\text{O}$) and palladium(II) chloride (PdCl_2) (Aldrich). Carbon monoxide (99.8%) was procured from Matheson.

All potentials are quoted vs. the saturated calomel electrode (SCE) and all measurements were made at room temperature, 23 ± 1 °C.

Results

The procedure for electrodeposition of platinum onto gold was in part similar to that given in ref 5a and b. This utilized a quiescent solution of 1×10^{-4} M H_2PtCl_6 in 0.5 M H_2SO_4 , the

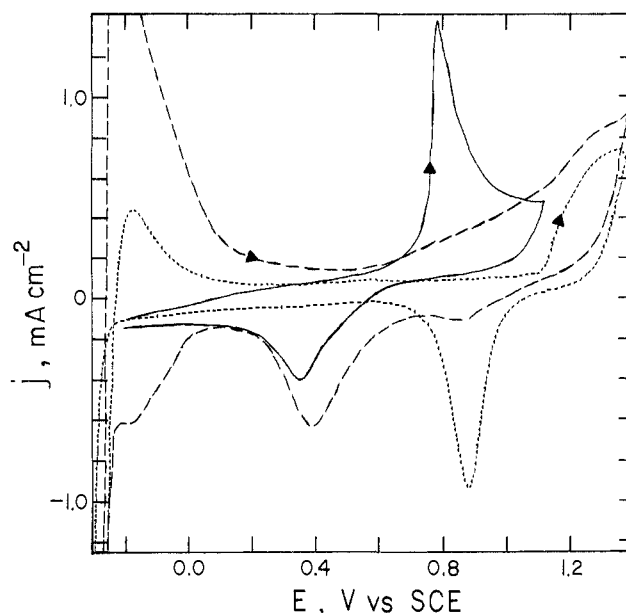


Figure 1. Anodic-cathodic cyclic voltammograms obtained in 0.5 M H_2SO_4 for (a) electrochemically roughened gold (dotted trace), (b) after platinum deposition (dashed trace), and for (c) after bubbling in CO (solid trace). Sweep rates: (a and b), 0.1 V s^{-1} , (c) 0.05 V s^{-1} . See text for conditions and for details of platinum electrodeposition.

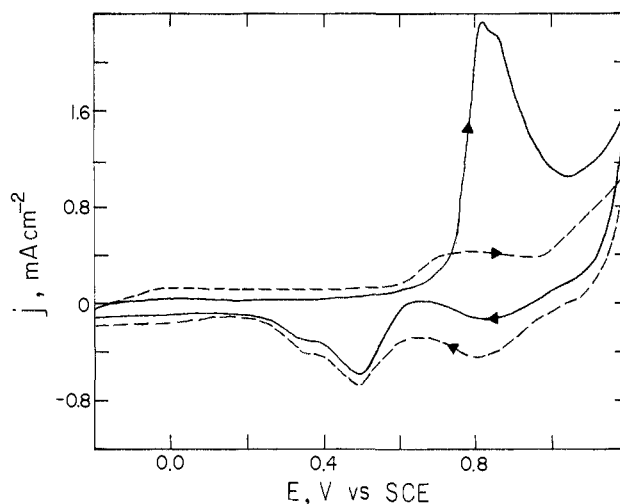


Figure 2. Anodic-cathodic cyclic voltammograms obtained at 0.1 V s^{-1} for electrochemically roughened gold electrode with electrodeposited palladium in 0.1 M HClO_4 (dashed trace) and after bubbling in CO (solid trace). See text for details of palladium electrodeposition.

electrode potential being held at 0.15 V vs. SCE for ≤ 2 min. The electrode was then transferred to 0.5 M H_2SO_4 for electrochemical and SERS characterization. Typical cyclic voltammograms obtained for the roughened gold electrode both before and after platinum deposition are shown in Figure 1. The characteristic anodic–cathodic voltammogram arising from the formation and removal of gold oxide (dotted trace), especially the AuO reduction peak at ca. 0.9 V, are replaced upon Pt deposition by corresponding features reminiscent of conventional platinum electrodes,¹³ with the PtO reduction yielding a broader cathodic wave around 0.4 V (dashed trace). The extent of these differences increased with the faradaic charge, q_f , passed during electrodeposition. The voltammogram shown in Figure 1 is for a q_f value of 1.5 mC cm^{-2} , corresponding to a surface concentration of deposited platinum, Γ , around $4 \times 10^{-9} \text{ mol cm}^{-2}$, i.e., about two equivalent monolayers. Values of q_f equal to or greater than ca. 1.5 mC cm^{-2} were usually required to suppress the AuO feature, thus indicating that the

(6) Sheppard, N.; Nguyen, T. T. In *Advances in Infrared and Raman Spectroscopy*; Clark, R. J. H., Hester, R. E., Eds.; Heyden: London, 1978; Vol. 5, p 67.

(7) Tadayyoni, M. A.; Weaver, M. J. *Langmuir* **1986**, *2*, 179.

(8) For a review, see: Bewick, A.; Pons, S. In *Advances in Infrared and Raman Spectroscopy*; Clark, R. J. H., Hester, R. E., Eds.; Heyden: London, 1985; Vol. 12, Chapter 1.

(9) Corrigan, D. S.; Gao, P.; Leung, L.-W. H.; Weaver, M. J. *Langmuir* **1986**, *2*, 744.

(10) Desilvestro, J.; Weaver, M. J. *J. Electroanal. Chem.* **1986**, *209*, 377.

(11) Tadayyoni, M. A.; Farquharson, S.; Li, T. T.; Weaver, M. J. *J. Phys. Chem.* **1984**, *88*, 4701.

(12) Corrigan, D. S.; Weaver, M. J. *J. Phys. Chem.* **1986**, *90*, 5300.

(13) For example, Rand, D. A. J.; Woods, R. J. *Electroanal. Chem.* **1972**, *35*, 209.

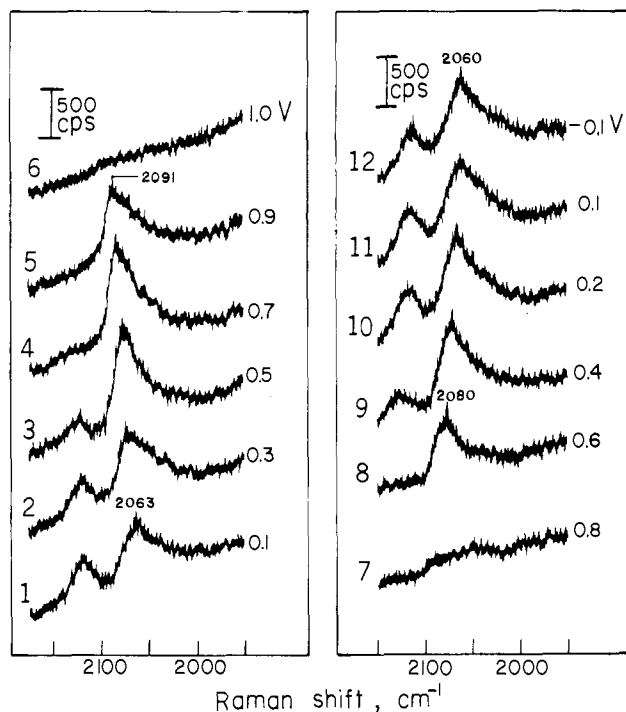


Figure 3. Potential-dependent SERS spectra in C–O stretching, ν_{CO} , region for CO adsorbed on a platinum-coated gold electrode. Electrolyte was 0.5 M H_2SO_4 saturated with CO. Spectra were obtained at the indicated potentials (vs. SCE) sequentially as numbered. Laser excitation was 50 mW at 647.1 nm; monochromator scan rate was $0.5 \text{ cm}^{-1} \text{ s}^{-1}$.

surface is covered mostly by platinum atoms. Once formed, the deposited surfaces yielded stable voltammetric behavior over long time periods (ca. 4 h) and repeated potential scans. Very similar voltammetric behavior was observed when using unroughened gold electrodes.

Comparable effects were observed upon the electrodeposition of palladium onto gold. The electrodeposition involved holding the electrode at 0.1 V in a solution of $5 \times 10^{-4} \text{ M PdCl}_2$ in 1 M HClO_4 . Figure 2 shows a typical cyclic voltammogram for a palladium-coated gold electrode in 0.1 M HClO_4 (dashed trace) formed with a q_f value of 2.0 mC cm^{-2} , corresponding to $\Gamma \approx 1 \times 10^{-8} \text{ mol cm}^{-2}$, i.e., about five equivalent monolayers. This film appears to be somewhat less uniform than for platinum in that the residual AuO reduction feature (Figure 2) was typically still present for such larger Γ values. Nevertheless, the voltammetric features characteristic of palladium oxide formation and reduction¹³ are clearly present (Figure 2).

The addition of carbon monoxide, by bubbling through the previously nitrogen-purged solution for a few minutes, yielded comparable voltammetric behavior for CO electrooxidation on these surfaces as is observed at bulk platinum and palladium electrodes.^{14,15} Typical anodic-cathodic voltammograms for CO-containing solutions are shown as solid traces in Figures 1 and 2. In both cases a sharp onset of anodic current, corresponding to CO electrooxidation, is seen at potentials close to the initial formation of platinum or palladium oxide. Similar observations for platinum overlayers on gold have been reported previously.^{5b,d}

Most notably, these platinum- and palladium-coated gold surfaces yielded well-defined SERS spectral features for adsorbed CO. Typical spectra in the ν_{CO} frequency region for CO adsorbed on the former surface are shown in Figure 3. The spectra shown were obtained after CO dosage in the numbered sequence shown, starting from the least positive potential (bottom left-hand spectrum) through a series of progressively more positive values and then returning to more negative potentials. The SERS features observed are stable over the extended periods of time (up

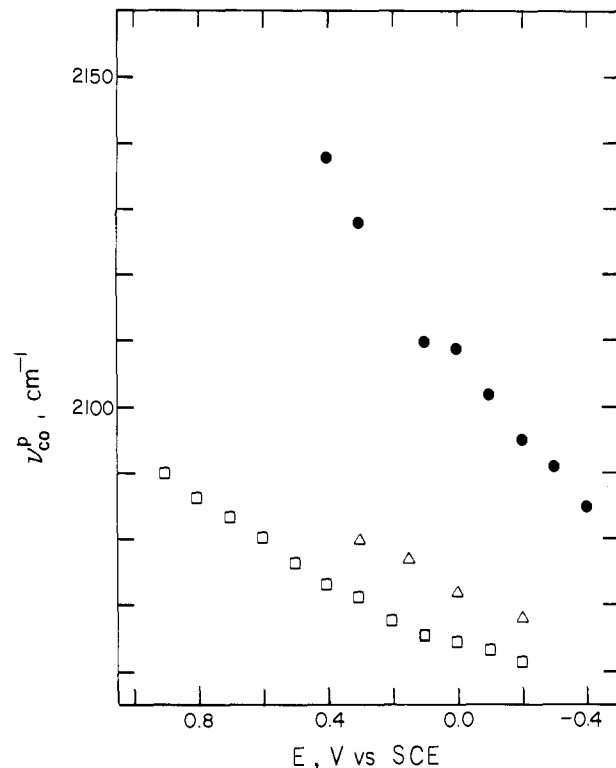


Figure 4. Peak frequency of SERS C–O stretching mode, ν_{CO}^p , for CO adsorbed on gold (filled circles) and platinum-coated gold (squares) as a function of electrode potential (conditions as in Figure 3). Also shown are ν_{CO} values obtained for CO adsorbed on platinum in 1 M HClO_4 (triangles) as obtained by PM-IRRAS, taken from ref 17a.

to 4 h) that were often required to obtain a comprehensive data set.

Two ν_{CO} bands are obtained, a weak feature at about 2115–2130 cm^{-1} and a stronger band at about 2060–2090 cm^{-1} , both having peak frequencies that increase toward more positive potentials. The intensity of the latter band was typically around 10^3 counts per second above background even at the low laser powers (ca. 50 mW) that were typically employed. The higher frequency band is identified with CO bound to residual uncovered gold sites. Thus, somewhat more intense bands in this frequency range are obtained for CO adsorbed at unmodified gold electrodes,⁷ whose intensity decreases markedly for the platinum-coated surfaces. Another feature indicative of this assignment is that the high-frequency ν_{CO} band disappears positive of 400 mV, consistent with the behavior seen on uncoated gold that reflects the facile CO electrooxidation kinetics on this surface.⁷ The lower frequency ν_{CO} band remains at an approximately constant intensity until 0.9 V, disappearing at more positive potentials but reappearing at 0.6 V when the potential is readjusted in a negative direction (Figure 3). Although the band remains upon removing the solution CO by purging with nitrogen, it is irreversibly lost by altering the potential to 1.0 V. The maximum intensity of this lower frequency band was obtained for electrodes with platinum deposits corresponding to ca. two equivalent monolayers. Although the high-frequency band could be eliminated using thicker platinum films, the intensity of the lower frequency feature was also diminished under these conditions.

The frequencies of this major ν_{CO} band in Figure 3, 2060–2090 cm^{-1} , are consistent with CO bound to surface platinum atoms in a terminal (“linear”) configuration.⁶ The significantly lower frequencies that are characteristic of CO bound in such a manner to platinum rather than gold surfaces can be attributed to the greater $d\pi$ metal–CO back-donation expected for the former.^{6,16} The peak frequencies of these bands, ν_{CO}^p , are plotted as a function of electrode potential in Figure 4. The closed circles and open

(14) (a) Breiter, M. W. *J. Electroanal. Chem.* **1979**, *101*, 329. (b) McCallum, C.; Pletcher, D. *J. Electroanal. Chem.* **1976**, *70*, 277.
(15) Breiter, M. W., *J. Electroanal. Chem.* **1980**, *109*, 243.

(16) Nakamoto, K. *Infrared and Raman Spectra of Inorganic and Coordination Compounds*, 4th ed.; Wiley: New York, 1986; p 291.

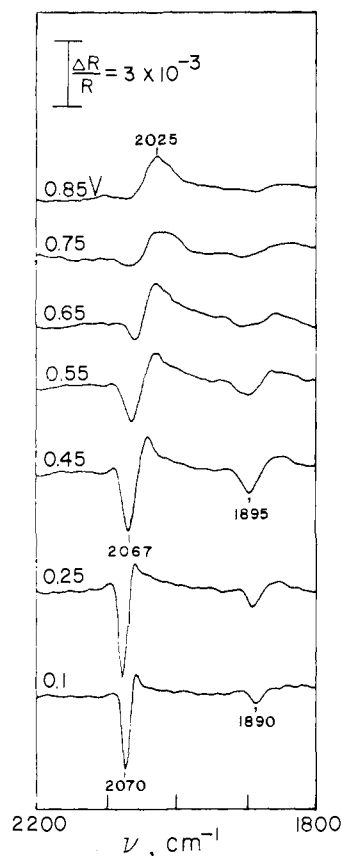


Figure 5. Potential-difference infrared (PDIR) spectra in ν_{CO} frequency region for CO adsorbed on a platinum-coated gold electrode. Electrolyte was 0.1 M H_2SO_4 saturated with CO. Spectra were obtained by obtaining 100 interferometer scans (requiring ca. 1 min) at the base (reference) potential, -0.2 V vs. SCE, and after stepping to the various sample potentials indicated, the former scans being subtracted from the latter. The spectral thin-layer cavity was re-formed between each pair of spectral scans.

squares denote the SERS $\nu_{\text{CO}}^{\text{P}}$ values for the higher and lower frequency bands, respectively, on the platinum-coated surface. Essentially the same $\nu_{\text{CO}}^{\text{P}}$ values were obtained for the latter band irrespective of the electrode potential history. Also plotted in Figure 4 are the potential-dependent $\nu_{\text{CO}}^{\text{P}}$ values obtained for CO adsorbed at platinum electrodes by using polarization-modulation infrared reflection absorption spectroscopy (PM-IRRAS), taken from ref 17a. The SERS and infrared $\nu_{\text{CO}}^{\text{P}}$ frequencies are seen to be reasonably close (within ca. 10 cm^{-1}) on these two types of platinum surface and display a comparable dependence upon electrode potential (ca. $30\text{ cm}^{-1}\text{ V}^{-1}$).

A more direct comparison between the SERS and infrared properties of this system was made by obtaining potential-difference infrared (PDIR) spectra in the ν_{CO} frequency region for CO adsorbed at platinum-coated gold under conditions identical with those utilized for the SERS measurements. A typical set of PDIR spectra for this system is shown in Figure 5. These were obtained by first recording 100 interferometer scans at the "base" potential, -0.2 V, stepping the potential to a more positive ("sample") value where another 100 spectral scans were obtained, and subtracting the first from the second set. The thin layer was re-formed between each pair of spectral measurements by retracting the electrode in order to replenish the CO solution in the spectral cavity and then pushing it back up to the CaF_2 window. This potential-difference procedure subtractively normalizes out the otherwise-dominant effect of the solvent, instrument drift, and other interferences. It is similar to that employed conventionally in potential-difference infrared experiment using FTIR instru-

mentation (so-called SNIFTIRS¹⁸), except that only a *single* potential step is employed here rather than repeatedly modulating the potential between the base and sample values. Although this rapid single-step PDIR procedure is limited to systems, such as adsorbed CO, displaying unusually strong IR signals, it has the advantage of enabling irreversible as well as reversible potential-induced changes to be monitored. (This matter is described in detail elsewhere.¹⁹)

Since the PDIR data in Figure 5 are plotted as normalized transmittance ($\Delta R/R$), as is conventional,⁸ the negative- and positive-going bands correspond to the presence of CO adsorbed at the sample and base potentials, respectively. The frequencies of the former are closely similar to (within 5 cm^{-1} of) the corresponding SERS $\nu_{\text{CO}}^{\text{P}}$ values in Figure 4, as well as to corresponding PDIR data obtained at a bulk platinum electrode.¹⁹ However, an interesting and surprising difference between the SERS and IR spectra in Figures 3 and 5 concerns the potential dependence of the ν_{CO} band intensities. The PDIR spectra (Figure 5) show the behavior anticipated from the voltammetric data (Figure 1) in that the negative-going ν_{CO} band disappears beyond ca. 0.7 V (Figure 5), close to the point where the anodic current commences for electrooxidation of solution CO (Figure 1). (This was confirmed by the corresponding appearance of a large negative-going band at 2340 cm^{-1} in the PDIR spectra due to the formation of solution CO_2 in this potential region.) In contrast, the ν_{CO} intensities in the corresponding SER spectra (Figure 3) do not decrease markedly until significantly more positive potentials, finally disappearing around 1.0 V.

This result becomes even more surprising when it is recognized that the time scale employed to obtain the single-potential-step PDIR spectra (ca. 1 min) is somewhat shorter than that required (ca. 2–4 min) in order to obtain each SER spectral scan. As expected, infrared spectra obtained using longer acquisition times, involving repeated potential alterations between the base and sample values ("multiple-step" PDIR, or SNIFTIRS), exhibited ν_{CO} bands that disappeared at slightly less positive values than observed in the single-step experiment. Consequently, the SERS-active adsorbed CO on the platinum surface exhibits a surprising resistance to electrooxidation at potentials where the infrared-active form undergoes essentially complete oxidation on a shorter time scale.

The SER and infrared spectral properties of CO adsorbed on the palladium-coated gold surface exhibit several features comparable to the corresponding platinum system. A typical set of SER spectra in the ν_{CO} -region for palladium-coated gold is shown in Figure 6. These were obtained in the same fashion as in Figure 3, except that 0.1 M HClO_4 rather than $0.5\text{ M H}_2\text{SO}_4$ was used as the supporting electrolyte. (Essentially the same SER spectra for the platinum surface were obtained using either media.) Two major ν_{CO} bands were observed on the palladium-coated surface, a feature around $2070\text{--}2090\text{ cm}^{-1}$ and a stronger band at $1965\text{--}1985\text{ cm}^{-1}$. The frequency of both features increases with increasing positive potential (Figure 6). By comparison with the interpretation of IR spectra obtained for palladium-gas interfaces,⁶ these high- and low-frequency ν_{CO} bands are identified with linear and bridge-bound CO, respectively. The latter, multiple-site, coordination geometry is known to be especially favored for palladium surfaces.⁶ The weak PDIR band observed at around $1880\text{--}1885\text{ cm}^{-1}$ on platinum-coated gold (Figure 5) is also indicative of this adsorption geometry, although the corresponding band was not detected in the corresponding SER spectra. The weak feature around $2120\text{--}2140\text{ cm}^{-1}$ seen for platinum-coated gold (Figure 3), due to CO adsorbed on residual gold sites, is less discernible on the palladium-coated surface, except after potential cycling over long time periods.

Figure 7 shows a corresponding set of PDIR spectra for CO adsorbed at the palladium-gold surface, recorded in the same

(17) (a) Russell, J. W.; Severson, M.; Scanlon, K.; Overend, J.; Bewick, A. *J. Phys. Chem.* **1983**, *87*, 293. (b) Kunimatsu, K.; Golden, W. G.; Seki, H.; Philpott, M. R. *Langmuir*, **1985**, *1*, 245.

(18) SNIFTIRS: subtractively normalized interfacial Fourier transform infrared spectroscopy.⁸

(19) Corrigan, D. S.; Leung, L.-W. H.; Weaver, M. J. *Anal. Chem.*, in press.

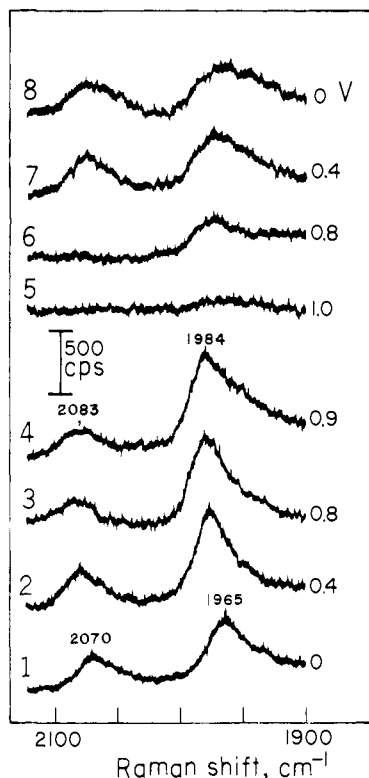


Figure 6. Potential-dependent SER spectra in ν_{CO} region for CO adsorbed on a palladium-coated gold electrode. Electrolyte was 0.1 M HClO_4 saturated with CO. Other details are as in caption to Figure 3.

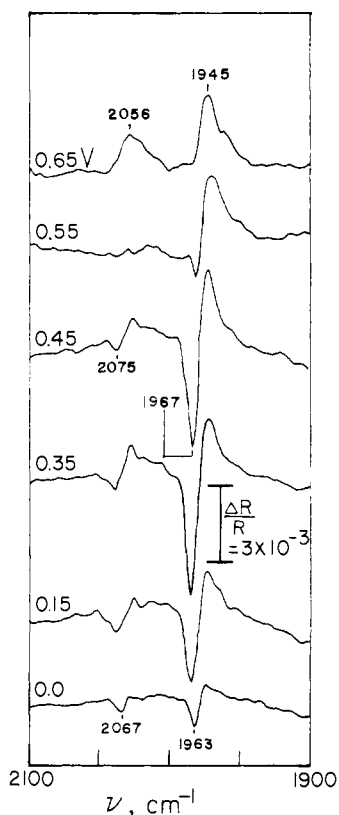


Figure 7. PDIR spectra in ν_{CO} frequency region for CO adsorbed on a palladium-coated gold electrode. Electrolyte was 0.1 M HClO_4 saturated with CO. Other details are as in footnote to Figure 5.

manner as in Figure 3. Infrared bands for both the terminal and bridge-bound forms are seen in Figure 7, with the latter being predominant. The relative intensities of these two bands are similar to those in the SER spectra (Figure 6). As for the platinum surface, reasonable agreement is also seen between the ν_{CO} fre-

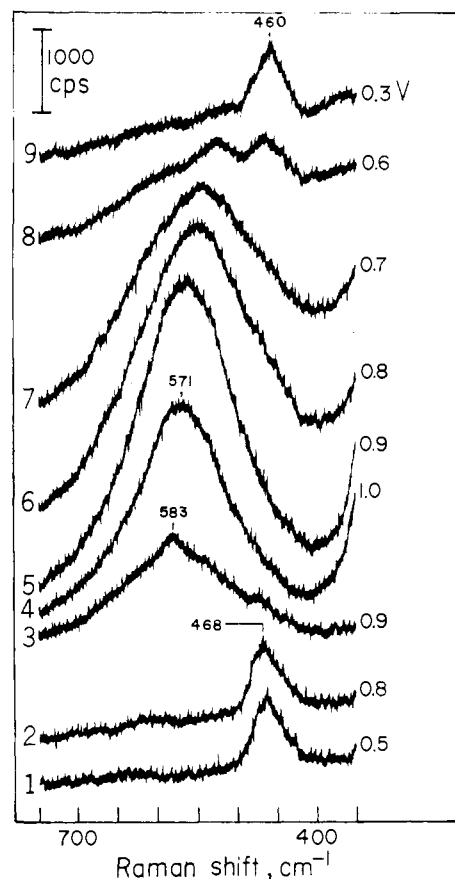


Figure 8. Potential-dependent SER spectra in low-frequency ($300\text{--}800\text{ cm}^{-1}$) region for a platinum-coated gold electrode in 0.5 M H_2SO_4 saturated with CO. Spectra were obtained at the indicated potentials (vs. SCE) sequentially as numbered. Laser excitation was 80 mW at 647.1 nm; monochromator scan rate was $0.5\text{ cm}^{-1}\text{ s}^{-1}$.

quencies of the corresponding bands in the SER and PDIR spectra, although the latter appear to shift with potential to a smaller extent than the former bands. The present IR spectra are also closely similar to those obtained for CO adsorbed at bulk palladium electrodes.²⁰

The potential dependence of the SERS and PDIR ν_{CO} band intensities on palladium-coated gold differ in a manner similar to that noted above for the platinum surface. Thus while the negative-going bands for both the terminal and bridge-bonded CO in the single-step PDIR spectra disappear entirely for sample potentials positive of 0.6 V, the corresponding SER bands survive until 0.9 V. The onset of electrooxidation of solution CO occurs at around 0.7–0.8 V on the voltammetric time scale (Figure 2). As for platinum, therefore, the SERS-active CO exhibits a significantly greater stability than the IR-active form toward electrooxidation.

The possible relation between CO electrooxidation and surface oxide formation can be explored by examining potential-dependent SER spectra in the low-frequency region. Figure 8 shows a series of such SER spectra between 300 and 800 cm^{-1} for platinum-coated gold in CO-saturated 0.5 M H_2SO_4 . These were recorded in the sequence as numbered, altering the potential first to more positive values into the region where platinum oxide is formed. The single band at about 460 cm^{-1} in the bottom spectrum, recorded at 0.5 V, is observed from -0.2 to 0.8 V in the presence of CO. This is attributed to the platinum-carbon stretching mode, $\nu_{\text{Pt-C}}$, for adsorbed CO; a band at a similar frequency has been observed for CO on platinum using electron energy loss spectroscopy.²¹ Altering the potential to values positive of 0.8 V results in the loss of this feature and the appearance of a broader band

(20) (a) Kunimatsu, K. *J. Phys. Chem.* **1984**, *88*, 2195. (b) Solomun, T. *Ber. Bunsenges, Phys. Chem.* **1986**, *90*, 557.
(21) Gland, J. L.; Kollin, E. B. *Surf. Sci.* **1985**, *151*, 260.

centered at around 560–580 cm^{-1} , which becomes extremely intense by 1.0 V (Figure 8). The intensity also gradually increases with time. This band, which is also present in the absence of CO, is assigned to a Pt–O stretching vibration, ν_{PtO} , for the platinum oxide film present in this potential region. We have previously observed similar bands accompanying the formation of anodic oxide films on unmodified gold.¹⁰ The spectral features shown in Figure 8 can be assigned with confidence to adsorbate–surface bonds involving the platinum overlayer rather than to gold sites since the latter surface exhibits no SERS bands in the 300–800- cm^{-1} region under the conditions encountered in Figure 8. Readjusting the potential back to less positive values, around 0.6 V, leads to a sharp decrease in the intensity of the ν_{PtO} feature and the accompanying reappearance of both the ν_{PtC} (Figure 8) and ν_{CO} bands (Figure 3).

A surprising feature of the ν_{PtO} band is that it only appears at potentials, ca. 0.9 V, significantly more positive of the region where platinum oxide formation commences, ca. 0.65 V, as discerned from the voltammograms (Figure 1). This point was checked further by monitoring the quantity of platinum oxide formed under the conditions required for obtaining the SER spectra (3–4 min at each potential) by measuring the faradaic charge contained under the peak for subsequent voltammetric reduction. Substantial oxide formation on this time scale was obtained for potentials beyond 0.65 V, the coverage increasing until an apparent "saturation" is reached at about 1.0 V. In contrast to platinum, the palladium-coated gold surface did not exhibit any easily discernible SERS bands in the low-frequency region.

In addition to the platinum and palladium systems described here, we have recently observed intense SERS for CO adsorbed on several other transition-metal overlayers electrodeposited onto gold, including rhodium, and ruthenium. While some features of the SER (and corresponding PDIR) spectra for the latter are similar to the former systems, the behavior is more complex and appears to be influenced by the oxide formation that occurs over broad potential regions on these surfaces. The detailed results of these studies will be described elsewhere, along with an examination of SERS and IR spectra for alkene and alkyne adsorbates on such surfaces.

Discussion

We believe that the present results provide the first clear-cut experimental demonstration that intense SERS can be obtained for transition-metal surfaces in an electrochemical environment. A recent theoretical analysis based on electromagnetic considerations indicates that weak yet significant SER enhancements should occur on appropriately sized transition-metal particles.²² Indeed, several reports and claims of transition-metal SERS have appeared previously. Cooney et al.²³ reported weak Raman spectra for CO adsorbed on a platinumized (i.e., extremely rough) platinum electrode. Although not originally interpreted as such, some SER enhancement may be involved. While some claims of SERS for halides on platinum and palladium electrodes²⁴ appear to be erroneous,²⁵ more convincing evidence exists for large Raman enhancements on roughened β -palladium hydride electrodes.²⁶ Raman spectra have also been reported for adsorbates on several transition metals in vacuum and gas-phase environments,²⁷ in-

cluding β PdH surfaces,^{27d} although it is not clear that significant SER effects are involved with the large surface area samples used in the majority of these studies. A report of weak SERS for a platinum colloid system has also appeared.²⁸

The surface enhancement factors (SEF) for the present transition-metal overlayer systems are difficult to estimate accurately in the absence of CO coverage data. Given that similar SEF values (ca. 10^6) are typically found for adsorbates on the gold as well as silver surfaces employed in our laboratory,^{4b,29} and that the SER intensities for ν_{CO} on the platinum- and palladium-coated surfaces are comparable with those on unmodified gold, one might deduce that similar SEF values occur for the transition-metal systems. However, by taking into consideration that the CO coverage on gold is 0.1 or less,⁷ in contrast to the near-monolayer levels likely on platinum and palladium, leads to SEF estimates on the latter surfaces (ca. 10^5) that are around 10-fold less than on the former substrate.

The damping effect upon the Raman enhancement of separating an adsorbate from a SERS-active substrate by thin overlayers has been examined by Murray.³⁰ Her electromagnetic calculations, as well as some experimental data for thin gold films on silver,^{30a} indicate that substantial (around 5–10-fold) diminutions in SEF should occur with one to two monolayer thick spacer layers, especially for transition metals that exhibit strong interband absorption in the visible spectral region.³⁰ The apparent damping of the SEF observed for the present overlayer systems therefore appears to be in harmony with these considerations.

Information pertinent to this question is also provided by comparing the potential-dependent SER and IR spectral intensities. As noted above, there is a small yet significant range of electrode potentials for both the platinum and palladium surfaces over which the adsorbed CO sensed by the infrared spectra is rapidly oxidized, yet the SERS-active CO remains unreactive. The former probe is not associated with a significant degree of surface enhancement,^{8,12} so that the infrared intensities are insensitive to surface morphology⁹ and are more likely to arise from the preponderant adsorbate. These results therefore suggest that the SERS probe senses only a minority of the total ensemble of adsorbed CO molecules, having an unusually low propensity to undergo electrooxidation. The percentage of SERS-active to total CO adsorption sites can be estimated crudely as $\leq 5\%$ on both the platinum and palladium surfaces from the essentially complete disappearance of the PDIR ν_{CO} band (Figures 5 and 7) at potentials (0.9 and 0.7–0.9 V for Pt and Pd, respectively) at which the corresponding SERS ν_{CO} bands remain intact. Consequently, the actual SERS enhancement factor is probably substantially larger than the apparent values obtained by presuming that every adsorbed CO molecule contributes equally to the SERS signals. A similar conclusion has been reached for SERS on unmodified silver from the essentially complete quenching of the Raman signals upon deposition of small coverages of thallium.³¹

The lower reactivity of the SERS-active adsorbed CO toward electrooxidation in comparison with the IR-active species indicates that the former adsorbate experiences a significantly different environment, even though the nature of the surface bonding appears to be similar on the basis of their comparable ν_{CO} frequencies. This difference can be understood in terms of an electrooxidation pathway involving reaction between adsorbed CO and metal oxide (or hydroxide); such a mechanism has been considered for both electrochemical³² and gas-phase CO oxidation²¹ on platinum.

(22) Cline, M. P.; Barber, P. W.; Chang, R. K. *J. Opt. Soc. Am. B: Opt. Phys.* **1986**, *3*, 15.

(23) Cooney, R. P.; Fleischmann, M.; Hendra, P. J. *J. Chem. Soc., Chem. Commun.* **1977**, 235.

(24) Loo, B. H. *Solid State Commun.* **1982**, *43*, 349. Loo, B. H.; Lee, Y. G. *J. Electroanal. Chem.* **1984**, *163*, 401. Loo, B. H. *J. Phys. Chem.* **1983**, *87*, 3003.

(25) Tadayoni, M. A.; Gao, P.; Weaver, M. J. *J. Electroanal. Chem.* **1986**, *198*, 125.

(26) Fleischmann, M.; Graves, P. R.; Hill, I. R.; Robinson, J. *Chem. Phys. Lett.* **1983**, *95*, 322.

(27) For example: (a) Krasser, W.; Bechthold, P. S.; Kettler, U., *Fresenius Z. Anal. Chem.* **1983**, *314*, 319. (b) Parker, W. L.; Hexter, R. M.; Siedle, A. R. *Chem. Phys. Lett.* **1984**, *107*, 96. (c) Parker, W. L.; Siedle, A. R.; Hexter, R. M. *J. Am. Chem. Soc.* **1985**, *107*, 264. (d) Parker, W. L.; Siedle, A. R.; Hexter, R. M. *J. Catal.* **1986**, *99*, 482.

(28) Benner, R. E.; Von Raben, K. U.; Lee, K. C.; Owen, J. F.; Chang, R. K.; Laube, B. L. *Chem. Phys. Lett.* **1983**, *96*, 65.

(29) Weaver, M. J.; Farquharson, S.; Tadayoni, M. A. *J. Chem. Phys.* **1985**, *82*, 4867.

(30) (a) Murray, C. A. *J. Electron Spectros. Relat. Phenom.* **1983**, *29*, 371. (b) Murray, C. A. *J. Opt. Soc. Am. B: Opt. Phys.* **1985**, *2*, 1330.

(31) (a) Furtak, T. E.; Roy, D. *Phys. Rev. Lett.* **1983**, *50*, 1301. (b) Watanabe, T.; Yanagihara, N.; Honda, K.; Pettinger, B.; Moerl, L. *Chem. Phys. Lett.* **1983**, *96*, 649.

(32) For example: (a) Randin, J.-P. In *Encyclopedia of Electrochemistry of the Elements*; Bard, A. J., Ed.; Marcel Dekker: New York, 1976; Vol. 7, Chapter 1. (b) Bilmes, S. A.; Tacconi, N. R. De.; Arvia, A. J. *J. Electroanal. Chem.* **1984**, *164*, 129.

Platinum oxide formation in the vicinity of the SERS-active sites only commences at ca. 0.9 V in both the absence and presence of CO as seen from the appearance of the ν_{PtO} band (Figure 8). The disappearance of both the ν_{CO} and ν_{PtO} bands at potentials close to this point therefore suggests that the electrooxidation of the SERS-active CO involves reaction with nearby oxygen or hydroxide species which constitute the "PtO" film. Consistent with this interpretation is the observation that electrooxidative loss of the preponderant, infrared-active, adsorbed CO commences at potentials, ca. 0.7 V, close to the onset of oxide formation as sensed by voltammetry (vide supra).

The structural origin of the relative inertness of the SERS-active sites toward CO electrooxidation and oxide formation is unclear. However, examination of both the former³³ and latter³⁴ processes on low-index single-crystal platinum faces indicates that they are both sensitive to the surface stereochemistry, although a simple correlation between the onset potentials for CO and surface oxidation is not observed.³³

Concluding Remarks

The present results constitute novel evidence that the strategy of coating suitably roughened gold surfaces with molecularly thin

transition-metal films provides a means of obtaining surface Raman spectra for species adsorbed at the transition metal–solution interface with intensities that are comparable to those obtained for conventional SERS-active gold or silver electrodes. As such, then, this simple approach appears to provide a relatively general means by which SERS can be applied to a broad range of transition-metal systems. One inevitable limitation is that it is difficult to eliminate entirely the presence of adsorbate bound to exposed substrate rather than to overlayer sites. The approach may therefore be limited to the examination of adsorbates that bind more strongly to the transition-metal overlayer rather than to the underlying substrate.

Nevertheless, the unique advantages offered by SERS, especially the freedom from bulk-phase interferences and the availability of wide frequency ranges, provide persuasive reasons to consider utilizing this approach to examine reactive as well as stable adsorbates on transition-metal surfaces. The use of multichannel array detectors, in particular, should enable SERS to provide an interesting new means of examining electrocatalytic reaction pathways on transition-metal surfaces. Studies of this type, involving a range of other transition-metal overlayers and including gas-phase as well as electrochemical systems, are currently in progress in our laboratory.

Acknowledgment. Helpful FTIR expertise was provided by Dennis S. Corrigan. This work is supported by the National Science Foundation.

(33) Leger, J.-M.; Bedin, B.; Lamy, C.; Bilmes, S. *J. Electroanal. Chem.* **1984**, *170*, 305.

(34) Yamamoto, K.; Kolb, D. M.; Kotz, R.; Lehmpfuhl, G. *J. Electroanal. Chem.* **1979**, *96*, 233.

A New Series of Molecular Semiconductors: Phthalocyanine Radicals¹

P. Turek,[†] P. Petit,[†] J.-J. André,[†] J. Simon,^{*‡} R. Even,[‡] B. Boudjema,[±] G. Guillaud,[±] and M. Maitrot[±]

Contribution from Groupe de Recherches sur les Matériaux Moléculaires (G.R.I.M.M.), I.C.S., 67083 Strasbourg, France, E.S.P.C.I., 75231 Paris Cédex 05, France, and U.C.B., 69100 Villeurbanne, France. Received February 17, 1987

Abstract: The electrical properties of thin films and single crystals of bis(phthalocyaninato)lutetium (Pc₂Lu) and lithium monophthalocyanine (PcLi) have been determined. Undoped single crystals of Pc₂Lu show a room temperature conductivity of $6 \times 10^{-5} \Omega^{-1} \text{cm}^{-1}$, more than 6 orders of magnitude higher than that for standard divalent ion metallophthalocyanines (PcM: M = Cu, Ni, ...). The conductivity of Pc₂Lu thin films is of the same order of magnitude ($10^{-5} \Omega^{-1} \text{cm}^{-1}$), demonstrating that structural disorder is ineffective in creating deep charge carrier traps. Single crystals of PcLi are even more conductive ($2 \times 10^{-3} \Omega^{-1} \text{cm}^{-1}$), but thin film conductivities are drastically depressed (10^{-4} – $10^{-5} \Omega^{-1} \text{cm}^{-1}$). By comparing magnetic and electrical properties of Pc₂Lu and PcLi, it has been shown that strong interunit interaction energy occurs in PcLi (bandwidth of the order of 1 eV), but it is weak in Pc₂Lu (50 meV). Dielectric spectra of Pc₂Lu thin films in the frequency range 10^{-3} – 10^4 Hz have permitted us to confirm the previous result that disorder does not create deep traps in Pc₂Lu. A space charge limited current model enabled us to calculate that the effective mobility of charge carriers is $\theta\mu = 1.3 \text{ cm}^2/(\text{V}\cdot\text{s})$ for thin films of Pc₂Lu. This is the highest value ever found for thin films of a molecular material at room temperature.

Inorganic materials with conductivities intermediate between those of metals and those of insulators form a homogeneous class of materials possessing a low density of intrinsic charge carriers associated with high mobilities and a temperature activated conductivity. These materials may be p- or n-doped and may be used to form junctions and associated electronics devices such as photoconductors or field effect and bipolar transistors. Many attempts have been made to obtain similar characteristics with molecular compounds.^{2–4} While intermediate conductivities very often have been encountered, members of the molecular family

show very disparate properties; in particular, the chemical processes involved in the charge transport and in the formation of junctions were not known in detail. The object of the present paper is to give a precise definition of molecular semiconductors and to describe two members of a new series of molecular semiconductors.

(1) Part 2. Part 1: Maitrot, M.; Guillaud, G.; Boudjema, B.; André, J. J.; Strzelecka, H.; Simon, J.; Even, R. *Chem. Phys. Lett.* **1987**, *133*, 59. Work carried out in the Groupe de Recherches Interdisciplinaires sur les Matériaux Moléculaires (G.R.I.M.M.).

(2) Meier, H. *Organic Semiconductors*; Verlag Chemie: Berlin, 1974.

(3) Gutmann, F.; Lyons, L. E. *Organic Semiconductors*; J. Wiley & Sons: New York, 1967.

(4) Simon, J.; André, J.-J. *Molecular Semiconductors*; Springer Verlag: Berlin, 1985.

[†] I.C.S.
[‡] E.S.P.C.I.
[±] U.C.B.